Preprints of the 21st IFAC World Congress (Virtual)
Berlin, Germany, July 12-17, 2020

Probabilistic Intent Inference for Predicting the Compliance with COLREGs between Two Surface Ships

Yonghoon Cho * **Jonghwi Kim** * **Jinwhan Kim** *

* *Department of Mechanical Engineering, KAIST, Daejeon, Korea (e-mail: {yhcho88, stkimjh, jinwhan}@kaist.ac.kr)*

Abstract: The international regulations for preventing collisions at sea (COLREGs) are the rules of the road for marine surface vessels. However, certain ships fail to comply with COLREGs and their non-compliance poses a greater danger to the maritime safety. This study proposes a probabilistic model for intent inference of ship maneuvers which consist of an intent model, a dynamics model, and a measurement model. An algorithm based on the proposed graphical model is implemented to infer and predict the ship's intent of non-compliance/compliance with COLREGs, which enables making proper decisions for collision avoidance maneuvers even when the opponent ship violates the marine traffic rules. In order to demonstrate the feasibility of the proposed algorithm, the results of extensive traffic simulations are presented and discussed.

Keywords: Unmanned surface vessels, COLREGs, Intent inference, Graphical model.

1. INTRODUCTION

Ship collisions are the most frequent marine accidents, and they have been notorious for having a high casualty rate because of their destructive nature. As a result, the International Maritime Organization (IMO) implemented the Convention on the International Regulations for Preventing Collisions at Sea (COLREGs), consisting of a series of regulations that enforce safety measures in ship navigation and collision prevention (IMO (1972)). They provide the guidelines on maritime traffic safety such as who has priority between two encountered ships and how evasive maneuvers should be taken. However, these regulations are not always adhered to by all ships, and the violation of the regulations may lead to a dangerous situation, particularly when one ship expects the other ship to follow the rules but the other ship does not. Navigational safety can be improved by predicting the behavior of the ship in encounter and taking appropriate actions at the right time, and thus it is important to infer the traffic ship's intent of compliance/non-compliance to the rules.

Previous researches on intent inference from the vehicle's trajectories have been conducted in various fields such as air-traffic management (Yepes et al. (2007); Hwang and Seah (2008); Liu and Hwang (2011)) and ground vehicle control (Laugier et al. (2011); Liebner et al. (2013)). Several studies have been carried out in the maritime domain as well. Woerner et al. (2018) tried to quantify the violation/compliance using deterministic approaches with reference to case law (Woerner et al. (2018)). The generalized propagation model that can reflect the operator's intention was developed and applied to ship collision avoidance (Svec et al. (2013); Shah et al. (2014); Shah et al. (2016)).

In the authors' previous work, the intent inference of ship maneuvers was addressed (Cho and Kim (2017); Cho et al. (2018)). A graphical model driven by the control action of the ship in encounter was developed and a two-stage Kalman filter (TSKF) was introduced to estimate the control action. In this paper, the previous graphical model is further refined and extended by newly introducing a measurement model. This enables inferring the maneuver intent with no need for explicitly estimating control actions and system states. The proposed approach uses the Bayes' theorem and directed separation (d-separation) for representing the inferred intent in a probabilistic form. The probability of each intent is calculated using the random sampling based approach (RSBA). To verify the feasibility of the proposed algorithm, randomly encountered ship traffic simulations are conducted and the results are presented.

2. PROPOSED ALGORITHM

According to rules 5 and 7 of the COLREGs, every vessel should at all times maintain a proper look-out by all available means. Visual observation and the various navigational aids provide information regarding the presence of other vessels. However, they do not explicitly provide the maneuver intent of the other ships.

2.1 Belief of intent

In this study, the "own ship" is defined as the ship under control, whereas the other ship is defined as the "obstacle ship". Figure 1 represents the proposed graphical model for intent inference, constructed using a dynamic Bayesian network (Cho and Kim (2017); Cho et al. (2018)). Here, I, u, x, and z represent intent, action, state, and measurement, respectively. The proposed model is composed

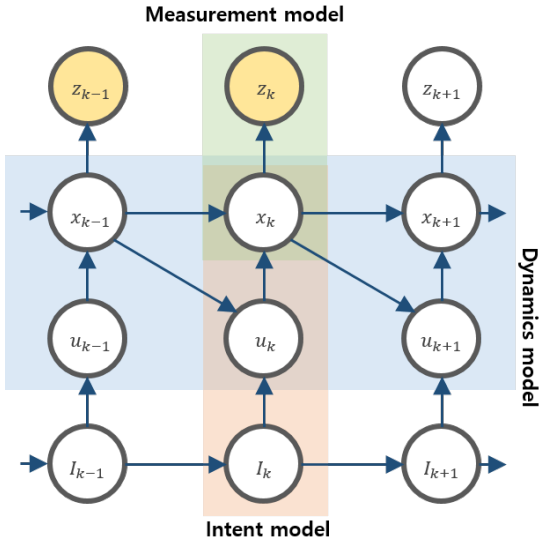

Fig. 1. Graphical model for intent inference with measurement model. I, u, x, and z represent intention, action, state, and measurement, respectively. Subscript refers to the time step. Red, blue, and green boxes represent intent model, dynamics model and measurement model, respectively. Yellow and white circles are the known variable and latent variable, respectively.

of three sub-models: an intent model, a dynamics model, and a measurement model. The intent model represents a human's behavior scheme wherein an intent leads to action which in turn changes the state. The dynamics model represents the evolution of the state due to the action. The measurement model represents the measurement generation from the state.

The probability of the estimated intent is represented as the belief of intent $bel\,(I_k)$. The measurement $\mathbf{z}$ is assumed to be given from time 1 to k, and then $bel\,(I_k)$ can be expressed as the probability of intent conditioned on the measurement from time 1 to k, as follows:

$$bel\,(I_k) = p(I_k|\mathbf{z}_{1:k}). \tag{2}$$

To calculate the $p(I_k|\mathbf{z}_{1:k})$, the state at the current step $\mathbf{x}_k$ is marginalized as follows:

$$p(I_k|\mathbf{z}_{1:k}) = \int_{\mathbf{x}_k} p(\mathbf{x}_k, I_k|\mathbf{z}_{1:k}) d\mathbf{x}_k, \tag{3}$$

where $p(\mathbf{x}_k, I_k|\mathbf{z}_{1:k})$ is described as the intended state probability, which can be calculated by (1). $I_k \in \{\mathcal{C}, \mathcal{V}\}$ is the intent set that can be considered by each ship: compliant intention, $\mathcal{C}$ and non-compliant intention, $\mathcal{V}$. As the ship cannot take both compliant and non-compliant actions simultaneously, the two types of intent are mutually exclusive. η_k is equal to $1/p(\mathbf{z}_k|\mathbf{z}_{1:k-1})$, which is used as a normalizer.

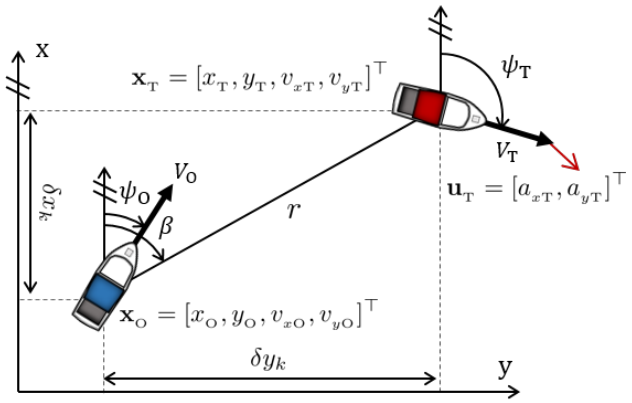

Fig. 2. Graphical representation of coordinates between the own ship (blue) and obstacle ship (red).

To represent the intended state probability to a familiar probabilistic form, Bayes' theorem is applied. Then, the marginalization of the previous state $\mathbf{x}_{k-1}$ and the current action $\mathbf{u}_k$, a chain rule of conditional probability, and d-separation are applied. By applying the d-separation, the conditionally independent variables are separated and the probabilities are expressed as follows:

$$\begin{aligned}
&p(\mathbf{z}_k|\mathbf{x}_k, I_k, \mathbf{z}_{1:k-1}) = p(\mathbf{z}_k|\mathbf{x}_k),\\
&p(\mathbf{x}_k|\mathbf{u}_k, \mathbf{x}_{k-1}, I_k, \mathbf{z}_{1:k-1}) = p(\mathbf{x}_k|\mathbf{u}_k, \mathbf{x}_{k-1}),\\
&p(\mathbf{u}_k|\mathbf{x}_{k-1}, I_k, \mathbf{z}_{1:k-1}) = p(\mathbf{u}_k|\mathbf{x}_{k-1}, I_k),\\
&p(I_k|\mathbf{x}_{k-1}, I_{k-1}, \mathbf{z}_{1:k-1}) = p(I_k|I_{k-1}).
\end{aligned} \tag{4}$$

The last equation in (1) comprises five probabilities consisting of measurement probability $p(\mathbf{z}_k|\mathbf{x}_k)$, state transition probability $p(\mathbf{x}_k|\mathbf{u}_k, \mathbf{x}_{k-1})$, intended action probability $p(\mathbf{u}_k|\mathbf{x}_{k-1}, I_k)$, intent transition probability $p(I_k|I_{k-1})$ and intended state probability at the previous step $p(\mathbf{x}_{k-1}, I_{k-1}|\mathbf{z}_{1:k-1})$. The intended state probability at the current step is recursively updated using the intended state probability at the previous step.

2.2 Modelling of probabilities

Figure 2 represents the coordinate system between the own ship and the obstacle ship. The state of the obstacle ship $\mathbf{x}_k$ is expressed as

$$\mathbf{x}_k = \left[x_{\mathrm{T},k}\ y_{\mathrm{T},k}\ v_{x\mathrm{T},k}\ v_{y\mathrm{T},k}\right]^\top, \tag{5}$$

where $x_{\mathrm{T},k}$ and $y_{\mathrm{T},k}$ are the position at time k in the north-east-down (NED) coordinate. $v_{x\mathrm{T},k}$ and $v_{y\mathrm{T},k}$ are

$$\begin{aligned}
p(\mathbf{x}_k, I_k|\mathbf{z}_{1:k}) &= \eta_k p(\mathbf{z}_k|\mathbf{x}_k, I_k, \mathbf{z}_{1:k-1}) p(\mathbf{x}_k, I_k|\mathbf{z}_{1:k-1})\\
&= \eta_k p(\mathbf{z}_k|\mathbf{x}_k) \iint_{\mathbf{x}_{k-1}, \mathbf{u}_k} p(\mathbf{x}_k|\mathbf{u}_k, \mathbf{x}_{k-1}, I_k, \mathbf{z}_{1:k-1}) p(\mathbf{u}_k, \mathbf{x}_{k-1}|I_k, \mathbf{z}_{1:k-1}) p(I_k|\mathbf{z}_{1:k-1}) d\mathbf{u}_k d\mathbf{x}_{k-1}\\
&= \eta_k p(\mathbf{z}_k|\mathbf{x}_k) \iint_{\mathbf{x}_{k-1}, \mathbf{u}_k} p(\mathbf{x}_k|\mathbf{u}_k, \mathbf{x}_{k-1}) p(\mathbf{u}_k|\mathbf{x}_{k-1}, I_k) p(\mathbf{x}_{k-1}, I_k|\mathbf{z}_{1:k-1}) d\mathbf{u}_k d\mathbf{x}_{k-1}\\
&= \eta_k p(\mathbf{z}_k|\mathbf{x}_k) \iint_{\mathbf{x}_{k-1}, \mathbf{u}_k} p(\mathbf{x}_k|\mathbf{u}_k, \mathbf{x}_{k-1}) p(\mathbf{u}_k|\mathbf{x}_{k-1}, I_k) \sum_{I_{k-1}} p(I_k|I_{k-1}) p(\mathbf{x}_{k-1}, I_{k-1}|\mathbf{z}_{1:k-1}) d\mathbf{u}_k d\mathbf{x}_{k-1}
\end{aligned} \tag{1}$$

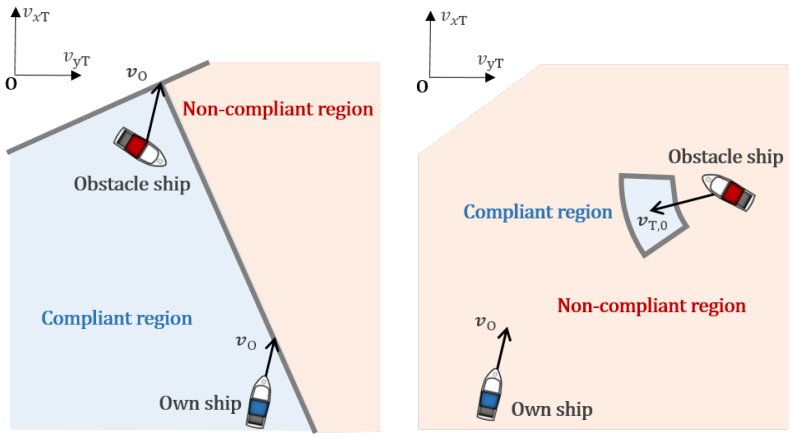

(a) Give-way (b) Stand-on

Fig. 3. Illustrations of compliant and non-compliant velocities in give-way and stand-on situations: The blue ship represents the own ship and the red ship is the obstacle ship.

the velocities along the NED coordinates. The action of the obstacle ship $\mathbf{u}_k$ is expressed as

$$\mathbf{u}_k = \left[a_{x\mathrm{T},k} \;\; a_{y\mathrm{T},k}\right]^\top, \tag{6}$$

where $a_{x\mathrm{T},k}$ and $a_{y\mathrm{T},k}$ are the acceleration along the NED coordinates. Because the position of the obstacle ship can be observed, the measurement $\mathbf{z}_k$ is written as

$$\mathbf{z}_k = \left[x_{\mathrm{T},k} \;\; y_{\mathrm{T},k}\right]^\top. \tag{7}$$

The measurement model is designed using the Gaussian distribution and can be written as

$$p(\mathbf{z}_k|\mathbf{x}_k) \sim \mathcal{N}\left(\mathbf{z}_k; H\mathbf{x}_k, R_k\right), H = \begin{bmatrix} 1 & 0 & 0 & 0 \\ 0 & 1 & 0 & 0 \end{bmatrix}. \tag{8}$$

Here, the measurement from the onboard sensor is generally provided by the range $r_k = \sqrt{(\delta x_k^2 + \delta y_k^2)}$ and bearing $\beta_k = \tan^{-1}(\delta y_k / \delta x_k)$. The covariance R_k with respect to the range and bearing can be written using Jacobian mapping as follows:

$$R_k = \begin{bmatrix} \cos\beta_k & -r_k \sin\beta_k \\ \sin\beta_k & r_k \cos\beta_k \end{bmatrix} \begin{bmatrix} \sigma_r^2 & 0 \\ 0 & \sigma_\beta^2 \end{bmatrix} \begin{bmatrix} \cos\beta_k & \sin\beta_k \\ -r_k \sin\beta_k & r_k \cos\beta_k \end{bmatrix}, \tag{9}$$

where σ_r and σ_β are the standard deviations of the range and bearing measurement.

The state transition probability is designed by an acceleration model with Gaussian white noise, written as

$$p(\mathbf{x}_k|\mathbf{u}_k, \mathbf{x}_{k-1}) \sim \mathcal{N}\left(\mathbf{x}_k; A\mathbf{x}_{k-1} + B\mathbf{u}_k, Q_k\right),$$

$$A = \begin{bmatrix} 1 & 0 & dt & 0 \\ 0 & 1 & 0 & dt \\ 0 & 0 & 1 & 0 \\ 0 & 0 & 0 & 1 \end{bmatrix}, B = \begin{bmatrix} 0 & 0 \\ 0 & 0 \\ dt & 0 \\ 0 & dt \end{bmatrix}, \tag{10}$$

where dt is the time difference between each step and Q_k is the covariance. The sub-covariance in velocity Q_k^v is calculated using Jacobian mapping with respect to speed $V_k = \sqrt{(v_{x\mathrm{T},k}^2 + v_{y\mathrm{T},k}^2)}$ and course $\psi_k = \tan^{-1}(v_{y\mathrm{T},k}/v_{x\mathrm{T},k})$ as follows:

$$Q_k^v = \begin{bmatrix} \cos\psi_k & -V_k \sin\psi_k \\ \sin\psi_k & V_k \cos\psi_k \end{bmatrix} \begin{bmatrix} \sigma_V^2 & 0 \\ 0 & \sigma_\psi^2 \end{bmatrix} \begin{bmatrix} \cos\psi_k & \sin\psi_k \\ -V_k \sin\psi_k & V_k \cos\psi_k \end{bmatrix}, \tag{11}$$

where σ_V and σ_ψ are the standard deviations of the model speed and course.

The probability of intent can be expressed by the probability mass function with two discrete random variables: compliant and non-compliant. The intent transition probability $p(I_k|I_{k-1})$ is represented as a transition probability matrix whose steady-state probability is equal for all elements.

Intended action probability $p(\mathbf{u}_k|\mathbf{x}_{k-1}, I_k)$, which represents the probability distribution for the next action based on the intent at the previous state, depends on the situation classified by COLREGs (Cho et al. (2019)). Figure 3 shows the desired velocities to be taken in a give-way and stand-on condition. The intended action can be calculated from the desired velocities.

The maneuver of the stand-on ship is divided into several stages according to the situation. The stand-on case in the intended action model considers rule 17(a)(i), which describes an obligation of speed and course keeping, assuming that the distance between the two ships is greater than the ship length. However, as noted in the rule 17 (a)(ii), if the give-way ship does not maneuver appropriately, the stand-on ship is obliged to take an evasive action. In these situations, the give-way model in Fig. 3(a) can be applied to detect non-compliant maneuver. Each condition is classified using the configuration between the two ships according to rules 13 to 17 of COLREGs.

2.3 Non-parametric approach

To obtain the belief of each intent using the previous mentioned modeling method, a non-parametric approach based on random sampling is applied. Algorithm 1 shows the procedure of the proposed approach. Intended state $p(\mathbf{x}_k, I_k|\mathbf{z}_{1:k})$ is represented by the finite number of weighted particle $\mathbf{x}_k^{[m]}$, instead of the parametric form, and $\mathcal{X}_k$ represents the set of particles. Each particle has intent $I_k^{[m]}$ with importance factor $w_k^{[m]}$, which can be interpreted as the weight of each particle.

In the proposed procedure, the intent at each particle is transited from time step $k-1$ to the next time step k

Algorithm 1 RSBA($\mathcal{X}_{k-1}, \mathbf{z}_k, p(I_k|I_{k-1})$)

$\bar{\mathcal{X}}_k = \mathcal{X}_k = \emptyset$
for $m = 1$ to M **do**
  sample $I_k^{[m]} \sim p(I_k|I_{k-1}^{[m]})$
  sample $\mathbf{u}_k^{[m]} \sim p(\mathbf{u}_k|I_k^{[m]}, \mathbf{x}_{k-1}^{[m]})$
  sample $\mathbf{x}_k^{[m]} \sim p(\mathbf{x}_k|\mathbf{u}_k^{[m]}, \mathbf{x}_{k-1}^{[m]})$
  $w_k^{[m]} = p(\mathbf{z}_k|\mathbf{x}_k^{[m]}) w_{k-1}^{[m]}$
  $\bar{\mathcal{X}}_k = \bar{\mathcal{X}}_k + < \mathbf{x}_k^{[m]}, w_k^{[m]}, I_k^{[m]} >$
end for
for $m = 1$ to M **do**
  $w_k^{[m]} = \text{NORMALIZE}(w_k^{[m]})$
end for
$\mathcal{X}_k = \text{RESAMPLE}(\bar{\mathcal{X}}_k)$
Return $\mathcal{X}_k$

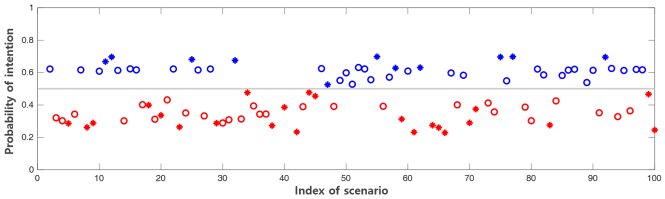

Fig. 4. The average probability of compliant intention. Blue represents the scenario with compliant intention, while red represents the scenario with violation intention. Circles and asterisks represent the encounter with give-way and stand-on obligation, respectively.

according to the intent transition probability. The action at each particle $\mathbf{u}_k^{[m]}$ is sampled using the intended action model $p(\mathbf{u}_k|I_k^{[m]}, \mathbf{x}_{k-1}^{[m]})$. The propagation from the state at particles $\mathbf{x}_{k-1}^{[m]}$ to that at the next step is implemented by using the state transition model $p(\mathbf{x}_k|\mathbf{u}_k^{[m]}, \mathbf{x}_{k-1}^{[m]})$. The weight of each particle $w_k^{[m]}$ is updated by $p(\mathbf{z}_k|\mathbf{x}_k^{[m]}) w_{k-1}^{[m]}$. Subsequently, each weight is normalized so that their sum is equal to one. To calculate the belief of intent, (3) is applied to the weighted particles. The belief of intent is equal to the summation of weight according to each intent and can be written as follows:

$$\begin{aligned} p(I_k = \mathcal{C}|\mathbf{z}_{1:k}) &= \sum_{i \in \{m | I_k^{[m]} = \mathcal{C}\}}^{M} w_k^{[i]}, \\ p(I_k = \mathcal{V}|\mathbf{z}_{1:k}) &= \sum_{i \in \{m | I_k^{[m]} = \mathcal{V}\}}^{M} w_k^{[i]}, \end{aligned} \tag{12}$$

where M is the number of particle.

3. SIMULATION RESULT

To validate the proposed algorithm, ship traffic simulations were conducted. Table 1 presents the settings for the RSBA for intent inference.

While simulating two ships that cross each other, the own ship observed and predicted the intention of the obstacle ship without taking action, while the obstacle ship took on non-compliant or compliant maneuver. Figure 4 shows the result of the average probability of compliant intention. The markers above the gray center line representing 0.5 probability are colored blue and the marker below the center line are colored red, which represents whether the obstacle ship intends to comply or violate the rules, respectively.

Figure 5 shows the estimated trajectories and probability of intention every 5 seconds. The color of the circular dots represents the probability of compliant intention and the location of dots represent the estimated position of obstacle ship in the body-fixed frame of the own ship. The estimated position can be calculated by the weighted sum of all the particle's position, written as:

$$p(\mathbf{x}_k|\mathbf{z}_{1:k}) = \sum_{I_k} p(\mathbf{x}_k, I_k|\mathbf{z}_{1:k}) = \sum_{m}^{M} w_k^{[m]} \mathbf{x}_k^{[m]}. \tag{13}$$

Most of the dots in non-compliant cases are red, while those in compliant cases are blue.

Table 2 shows the quantitative performance of intent inference using precision, recall and F_1 score which is defined as the harmonic mean of precision and recall. The probability of intention around 0.5 indicates that the intent inference algorithm cannot clearly identify the intention. Therefore, if 0.5 is defined as the neutral zone whose width is defined as p_m, the inferred intention can be written as

$$\text{Intent} = \begin{cases} \text{Compliant}, & \text{if } bel(I_k = \mathcal{C}) > 0.5 + p_m/2 \\ \text{Non-compliant}, & \text{if } bel(I_k = \mathcal{V}) > 0.5 + p_m/2 \\ \text{Neutral}, & \text{otherwise.} \end{cases} \tag{14}$$

As the p_m increases, the uncertain situation near 0.5 is inferred as neutral, so the precision increases, but the recall decreases, as shown in Table 2.

Table 1. Settings for RSBA

Parameter		Value
Number of particle (M)		10000
Sampling rate of measurement	[Hz]	1.0
Standard deviation of speed (σ_V)	[m/s]	0.2
Standard deviation of course (σ_ψ)	[deg.]	0.4
Standard deviation of measured range (σ_r)	[m]	5.0
Standard deviation of measured bearing (σ_β)	[deg.]	5.0

4. CONCLUSION

In this paper, the algorithm for the intent inference of COLREGs compliance has been presented. For this, the probabilistic model was constructed using a dynamic Bayesian model and the belief of intent was derived by the Bayes' rule, conditional probability, and d-separation. For calculating the belief of intent, each probability distribution was modeled and the random sampling based approaches were applied. The satisfactory performance of the proposed approach was observed from maritime traffic simulation results.

ACKNOWLEDGEMENTS

This research was supported by the project titled "Development of autonomous ship technology (development

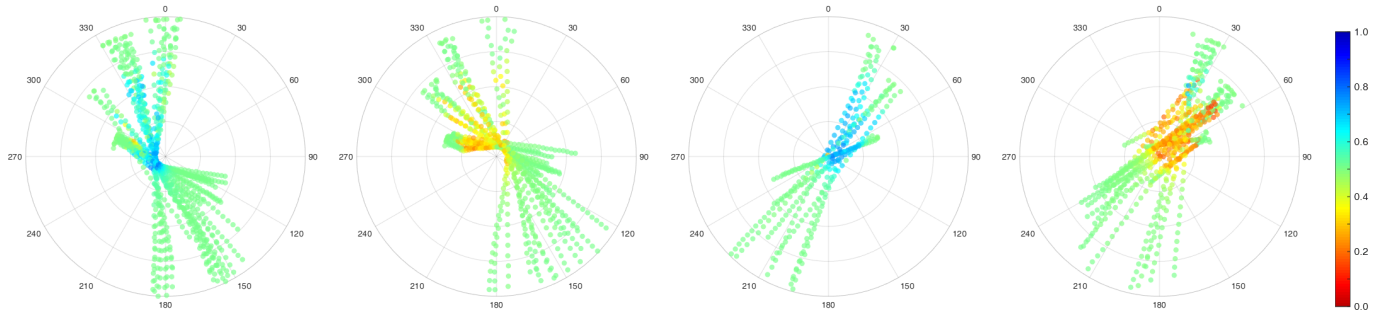

(a) Compliant in give-way situation (b) Non-compliant in give-way situation (c) Compliant in stand-on situation (d) Non-compliant stand-on situation

Fig. 5. The belief of compliant intention and estimated trajectory at each scenario. Circular dots are the relative position in the body-fixed coordinate of the observing ship. The color of the dots represents the belief of intention. The radius of the polar coordinates is 10.0 nmi.

Table 2. The quantitative performance of intent inference

	GIVE-WAY			STAND-ON			ALL		
Width (p_m)	Precision	Recall	F_1 score	Precision	Recall	F_1 score	Precision	Recall	F_1 score
0.00	0.8755	0.8755	0.8755	0.9825	0.9825	0.9825	0.8831	0.8831	0.8831
0.10	0.9524	0.7405	0.8332	0.9490	0.8280	0.8844	0.9511	0.7728	0.8527
0.20	0.9788	0.5965	0.7413	0.9826	0.7742	0.8660	0.9805	0.6622	0.7905

of autonomous navigation system with intelligent route planning function)", which is funded by the ministry of Oceans and Fisheries, Korea.

REFERENCES

Cho, Y., Han, J., and Kim, J. (2018). Intent inference of ship maneuvering for automatic ship collision avoidance. *IFAC-PapersOnLine*, 51(29), 384–388.

Cho, Y., Han, J., Kim, J., Lee, P., and Park, S.B. (2019). Experimental validation of a velocity obstacle based collision avoidance algorithm for unmanned surface vehicles. *IFAC-PapersOnLine*, 52(21), 329–334.

Cho, Y. and Kim, J. (2017). Collision probability assessment between surface ships considering maneuver intentions. In *OCEANS 2017-Aberdeen*, 1–5. IEEE.

Hwang, I. and Seah, C.E. (2008). Intent-based probabilistic conflict detection for the next generation air transportation system. *Proceedings of the IEEE*, 96(12), 2040–2059.

IMO (1972). COLREGS - International Regulations for Preventing Collisions at Sea. *Convention on the International Regulations for Preventing Collisions at Sea, 1972*.

Laugier, C., Paromtchik, I.E., Perrollaz, M., Yong, M., Yoder, J.D., Tay, C., Mekhnacha, K., and Nègre, A. (2011). Probabilistic analysis of dynamic scenes and collision risks assessment to improve driving safety. *IEEE Intelligent Transportation Systems Magazine*, 3(4), 4–19.

Liebner, M., Klanner, F., Baumann, M., Ruhhammer, C., and Stiller, C. (2013). Velocity-based driver intent inference at urban intersections in the presence of preceding vehicles. *IEEE Intelligent Transportation Systems Magazine*, 5(2), 10–21.

Liu, W. and Hwang, I. (2011). Probabilistic trajectory prediction and conflict detection for air traffic control. *Journal of Guidance, Control, and Dynamics*, 34(6), 1779–1789.

Shah, B.C., Švec, P., Bertaska, I.R., Klinger, W., Sinisterra, A.J., von Ellenrieder, K., Dhanak, M., and Gupta, S.K. (2014). Trajectory planning with adaptive control primitives for autonomous surface vehicles operating in congested civilian traffic. In *2014 IEEE/RSJ International Conference on Intelligent Robots and Systems*, 2312–2318. IEEE.

Shah, B.C., Švec, P., Bertaska, I.R., Sinisterra, A.J., Klinger, W., von Ellenrieder, K., Dhanak, M., and Gupta, S.K. (2016). Resolution-adaptive risk-aware trajectory planning for surface vehicles operating in congested civilian traffic. *Autonomous Robots*, 40(7), 1139–1163.

Svec, P., Shah, B.C., Bertaska, I.R., Alvarez, J., Sinisterra, A.J., Von Ellenrieder, K., Dhanak, M., and Gupta, S.K. (2013). Dynamics-aware target following for an autonomous surface vehicle operating under COLREGs in civilian traffic. In *2013 IEEE/RSJ International Conference on Intelligent Robots and Systems*, 3871–3878. IEEE.

Woerner, K., Benjamin, M.R., Novitzky, M., and Leonard, J.J. (2018). Quantifying protocol evaluation for autonomous collision avoidance. *Autonomous Robots*, 1–25.

Yepes, J.L., Hwang, I., and Rotea, M. (2007). New algorithms for aircraft intent inference and trajectory prediction. *Journal of guidance, control, and dynamics*, 30(2), 370–382.